

## Preparation of Cu, Ag, Fe and Al nanoparticles by the exploding wire technique<sup>†</sup>

P SEN\*, JOYEE GHOSH, ALQUDAMI ABDULLAH, PRASHANT KUMAR and VANDANA

School of Physical Sciences, Jawaharlal Nehru University,  
New Delhi 110 067, India  
e-mail: prasenjitsen@vsnl.net

**Abstract.** We describe a novel process for the production of nanoparticles of Cu, Ag, Fe and Al which involves exploding their respective wires, triggered by large current densities in the wires. The particles are characterised by X-ray diffraction (XRD) and atomic force microscopy (AFM). Particle sizes in the range 20–100 nm were obtained employing this technique. The XRD results reveal that the nanoparticles continue to retain lattice periodicity at reduced particle sizes, displaying in some cases evidence of lattice strain and preferential orientation. In the case of Fe, Mossbauer spectroscopy reveals loss of ferromagnetism as a result of the reduced size of the particles.

**Keywords.** Metallic nanoparticles; electro explosion of wires; atomic force microscopy.

### 1. Introduction

Nanoparticles have been a source of great interest due to their novel electrical, optical, physical, chemical and magnetic properties. They have significant potential for a wide range of applications such as catalysis, magnetic recording media, optoelectronic materials, magnetic fluids, composite materials, fuel cells, pigments and sensors. Their uniqueness arises from their high ratio of surface area to volume (aspect ratio), as these materials typically have diameters of 100 nm or less.

There are several reports of physical/chemical processes for the production of nanoparticles in technical literature. Nanoparticles prepared by physical methods such as vapour deposition and sputtering are of high quality, i.e., they possess clean surfaces and uniform particle size distribution. However, industrial applications for such particles are limited due to the low production rates and high cost. Alternative chemical production methods, such as thermal decomposition and precipitation are currently being studied for the preparation of a wide range of nanoparticles. Chemical methods can provide large quantities of ceramic particles for industrial applications. However, except for precious metals, chemical methods are generally not applied to the production of metallic nanoparticles. Thus to obtain metallic nanoparticles in large quantities novel methodologies need to be devised.

The phenomena of exploding wires (electro explosion of wires or EEW) have been widely used by plasma physicists for the generation and confinement of plasmas. Several

---

<sup>†</sup>Dedicated to Professor C N R Rao on his 70th birthday

\*For correspondence

parameters such as voltage, current pulse, material type and their wire dimension, and the medium in which the explosion is performed, etc. have a control on the entire process.

Employing this technique, underwater electric arcs have been shown<sup>1</sup> to cause strong explosions. With pulse current amplitudes of a few hundred amperes, the explosions are driven by electrodynamic forces, which scale with the square of the current.

Plasma formation from exploding individual wires and multiwire arrays, powered by a 450 kA, 100 ns pulsed power generator has been studied<sup>2</sup> with X-ray direct backlighting. The structure of the dense core plasmas for Fe wires is the same as for Ti wires. For Cu and Ni wires, similar to Ti, there is a sharp boundary between the dense core and coronal plasmas, and transverse and longitudinal structures are both seen within the dense cores.

Other materials like thin tungsten wires disintegrate in vacuum when they are electrically exploded.<sup>3</sup> The wires split into tiny fibres in time periods close to that at which the wire reaches its melting point. Similar results are obtained for wires exploded at low pressures and at atmospheric pressure. When the wire reaches its melting point hard X-rays are produced due to the splitting of the wire, which has a fibre-like crystalline structure.

Current-induced explosions of 7.5–25  $\mu\text{m}$  diameter metal wires show a persistent foam-like liquid–vapour structure of the expanded wire core. A substantial portion of the wire is not vaporised but remains in the condensed state. As the current damps out, the remaining liquid phase material coalesces into separate droplets. This is seen in W, Mo, NiCr and Ti wire explosions.<sup>4</sup> By contrast, Al, Au, Cu and Ag wires, all high conductivity materials, with relatively low melting points, form fully vaporized and more uniform expanding columns of wire, evidently because the energy deposited in them during the critical first 50 ns of the current pulse is sufficient to cause the multiphase condition to be short-lived.

Various theories<sup>5</sup> have been put forward to explain the electro dynamical changes that occur during the explosion of thin wires. The rupturing forces arise from the imbalance of the self-induced electromotive force and the ohmic potential during an explosive current surge, which account for the wire breaking into several segments.

The exploding wire phenomenon was described by Aspden<sup>6</sup> as to one which occurs owing to high current transients interacting with the self-inductive field within the wire, precluding the electron charge carriers from balancing the tensile stresses set up by the effect of the applied EMF on the positive ions of the wire structure.

Ivezia<sup>7</sup> has proposed that the longitudinal ponderomotive forces in current carrying conductors are not of magnetic but of electric origin. Thus these longitudinal electric forces, induced by ‘relativistic’ electric fields, explain the brittle tension breaks in the solid straight wire, which has been weakened by Joule heating.

With this background it is clear that explosion of wires create small fragments presumably due to condensation of the plasma state. It is thus of interest to see if these can be controlled to achieve particle sizes in the nanometre regime.

## 2. Methodology

### 2.1 Theoretical background

A simple background for the electro-explosion of wires has been presented by Graneau<sup>5</sup> who offers a theoretical explanation for this phenomenon, supporting his argument based on the axial forces expected to exist between separate elements of a current circuit

according to Ampere–Neumann electrodynamics as they apply to steady currents. Graneau effectively specified an open circuit condition by which isolated circuit elements are subject to axial forces generated by mutual action of current in different parts of the element. The force is of the form:

$$F = I^2 \log(L/D),$$

where  $I$  is the current in amperes and  $L/D$  is the ratio of the length of element  $L$  to a quantity  $D$  of the order of its thickness.

Graneau's hypothesis is that the fractures are tensile in character, whereas pinch forces that are generally observed during explosion are compressive and cannot cause wire fragmentation of the form observed. However his theoretical account does not explain why the wire breaks into as many as 50 fragments. Each of these fragments is of insufficient length to develop adequate force.

According to Aspden,<sup>6</sup> the most obvious cause for an axial force in the path of current flow is the direct action of electromotive force on charges in the conductor. When an EMF is applied to a conductor the field intensity  $E$  applies force to the electron population having mobility, which accounts for current flow. The forces impart momentum to the electrons, which is transferred by collision forces and is balanced by the action of  $E$  upon the positive charge of the atomic lattice. Overall, there is no resultant axial force on the conductor because the EMF and the potential drop determined by the collision-related ohmic losses are balanced. Thus, in the steady state current condition, the closed circuit flow involves no axial forces along the current path.

Now, when the EMF is changing owing to magnetic induction effects, including self-induction within the conductor, the applied EMF and the potential drop are no longer in balance. Their difference can be measured experimentally and can account for an axial force in the line of current flow. Under these conditions the positive atomic lattice of the conductor is subject to the full intensity  $E$ , as are the electrons, but the electrons have an additional role. They not only act as catalysts in transferring momentum to the lattice by collisions, but they also transfer momentum to whatever it acts on, as a store for the energy associated with the magnetic induction process. The field medium is closely coupled with the collective electron action and this field can assert forces in its interaction with charge in matter. In effect, therefore, we can reasonably expect a residual axial reaction force corresponding to the work done by the EMF in feeding energy into the self-conductance of the conductor when its current increases. The force is axial, acting between the conductor and the field induced in the observer's reference frame by the electron motion. Such a force can cause rupture of the conductor if the current build up is rapid enough, but it cannot separate the conductor body from the electron population. All that can be expected is that the conductor will disintegrate into elements, which are contained during the explosion within the plasma formed by the current discharge. The reason for this is that the force acting on each positive element of the atomic lattice of the conductor is not, in general, the same throughout the conductor. The quantitative analysis fully supports this explanation. According to Graneau<sup>5</sup>, the arguments based on electrodynamics require induced stress to be proportional to the square of current, whereas the new explanation suggested by Aspden involves a linear current relationship.

## 2.2 Experimental set-up

As mentioned before, in this technique, very high currents are passed through thin metallic wires in a very short time. The key factors for the control of EEW are the following.

- (1) The current  $I$  should be very large, i.e. very high current densities are required for the explosion process, which basically gives rise to some nonlinearity in the volt-ampere characteristics.
- (2) The initial stage of EEW is a Z-pinch (i.e., sudden reduction of the wire diameter at the point of explosion) which essentially decreases the cross-sectional area of contact to 1/100th of the rest of the conductor, thereby tremendously increasing the current density which is required for explosion to take place, whenever contact is made and broken.
- (3) A medium in which the explosion is to be performed.

In order to achieve explosions from the various wires, a reaction vessel was designed.<sup>8</sup> A wire is driven through a wire guide and exploded on a plate of the same material. Low DC voltages were employed to deliver a current until visible explosion was achieved.

The explosion was carried out in a dense medium, typically water or some heavy alcohol where the particles remain suspended and is collected in the following manner. An initial centrifuge of the suspension at 5000 RPM separates the fluid from the solid mass. While the former is rejected, the solid mass is dispersed in electronic grade acetone for further AFM analysis. AFM analysis was carried out employing the CP-R model of thermomicroscopes in the contact mode employing a silicon ultralever having a force constant of 0.2 N/m, USA. The contact force was set at 10<sup>-4</sup> nN for all topography data collected with the AFM. The nanoparticles dispersed in acetone are spread on single crystalline silicon (100).

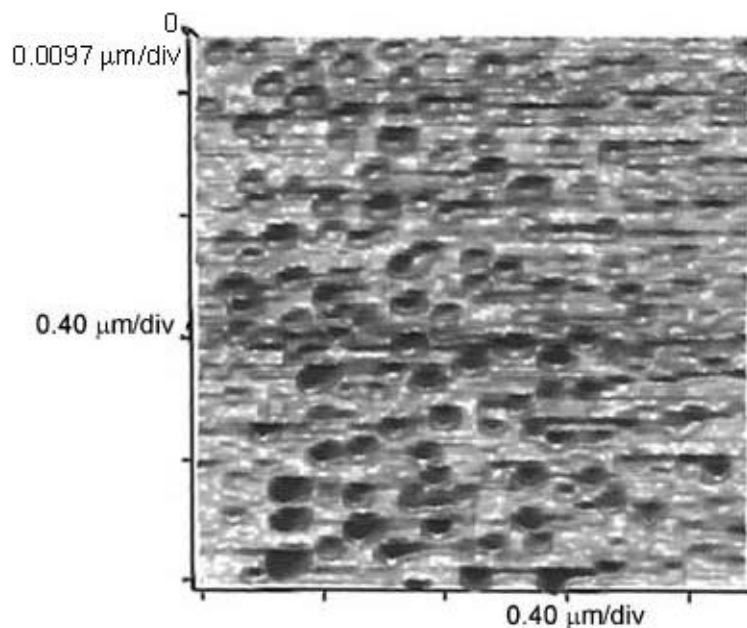
Part of the solid mass was incorporated in a paper matrix, dried and held firm for X-ray diffraction studies (XRD).

## 3. Results and discussion

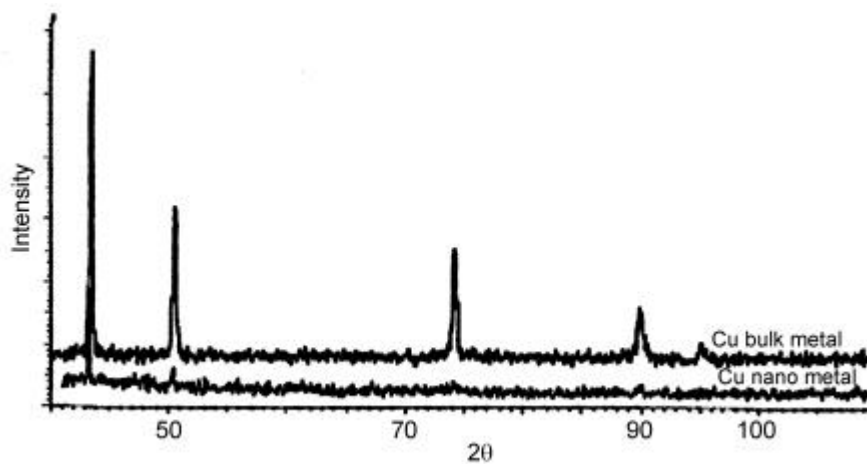
### 3.1 Copper

Figure 1 shows the 3-dimensional projection of AFM data collected for nano-crystalline copper particles dispersed on Si (100).<sup>8</sup> The AFM picture shows a uniform distribution of the particles, separated from each other, and there is no clustering seen as such. A typical particle is chosen for the size measurement by drawing a line across it, and the diameter measured. Several particles were investigated to infer particle sizes in the range 27–72 nm.

Figure 2 shows the XRD pattern recorded for bulk copper as a  $q$ - $2q$  plot scanning from 41–100° showing the lines (111), (200), (220), (311), (222) at  $2q$ = 43.44°, 50.50, 74.20°, 90.00°, and 95.10° respectively. For the copper nanoparticles, collected at 36 V and incorporated in the paper matrix as mentioned above, only one main peak at  $2q$ = 43.44° was observed. The observation of a diffraction peak for the copper nanoparticles indicate that these are still crystalline in this size range while its broadening is related to the reduced particle size. However, the predominance of the (111) line in XRD indicates reorientation of the nanoparticle grains preferentially in one direction as against the random orientation of grains in the bulk material.



**Figure 1.** A contact mode AFM picture of the copper nanoparticles as a 3-dimensional projection. The height axis (Z axis) is perpendicular to the plane of the paper.



**Figure 2.** X-ray diffraction pattern of bulk copper metal is compared with copper nanoparticles obtained by the EEW technique.

### 3.2 Silver

Figure 3 shows the 3-dimensional projection of AFM data collected for nano-crystalline silver particles dispersed on Si (100).<sup>8</sup> The AFM picture shows individual spherical particles, however, some clustering is observed as well. As above, several particles were

examined to infer particle sizes in the range 50–200 nm by drawing a line across the particles.

Figure 4 shows the XRD pattern recorded for bulk silver as a  $q$ - $2q$  plot scanning from  $38^{\circ}$ – $82^{\circ}$  generating the lines (111), (200), (220), (311), (222) at  $2q=38.144^{\circ}$ ,  $44.273^{\circ}$ ,  $64.470^{\circ}$ ,  $77.379^{\circ}$ , and  $81.500^{\circ}$  respectively. For the nano-silver sample held onto a paper matrix as stated above, an XRD pattern was generated as a  $q$ - $2q$  plot scanning from  $38^{\circ}$ – $82^{\circ}$  generating the lines (111), (200), (220), (311), (222) at  $2q=38.016^{\circ}$ ,  $44.182^{\circ}$ ,

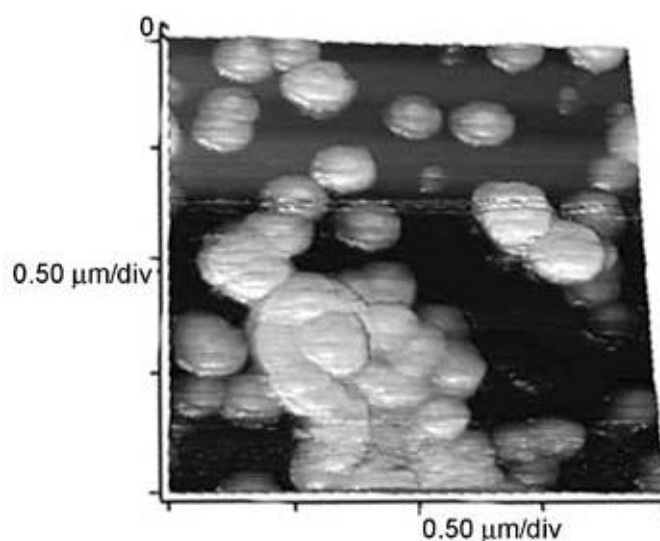


**Figure 3.** A contact mode AFM picture of the silver nanoparticles as a 3-dimensional projection. The height axis ( $Z$  axis) is perpendicular to the plane of the paper.

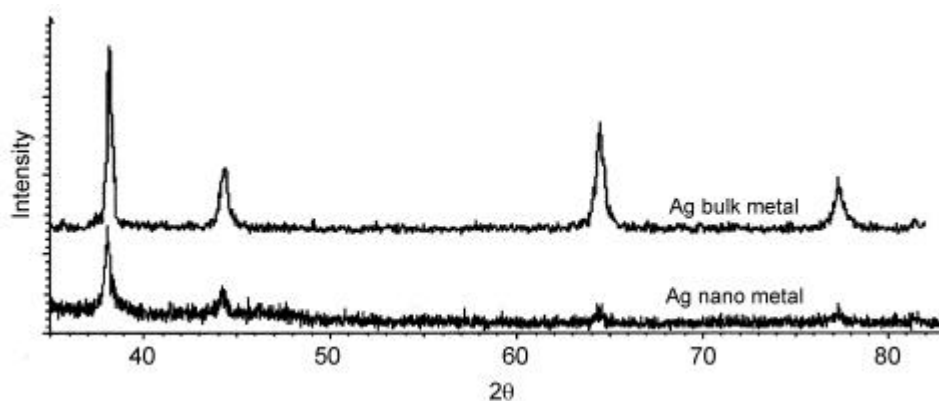


**Figure 4.** X-ray diffraction pattern of bulk silver metal is compared with silver nanoparticles obtained by the EEW technique.

64.351°, 77.317°, and 81.500° respectively. The position of these lines in XRD is similar to those obtained in bulk silver. This indicates the purity of the nanoparticle lattice having bulk-like periodicity in the particles investigated. Relative intensities of the lines have however altered showing re-orientation of grains following their production through the EEW method.



**Figure 5.** A contact mode AFM picture showing the iron nanoparticles as a 2-dimensional projection. The length of one edge is marked.

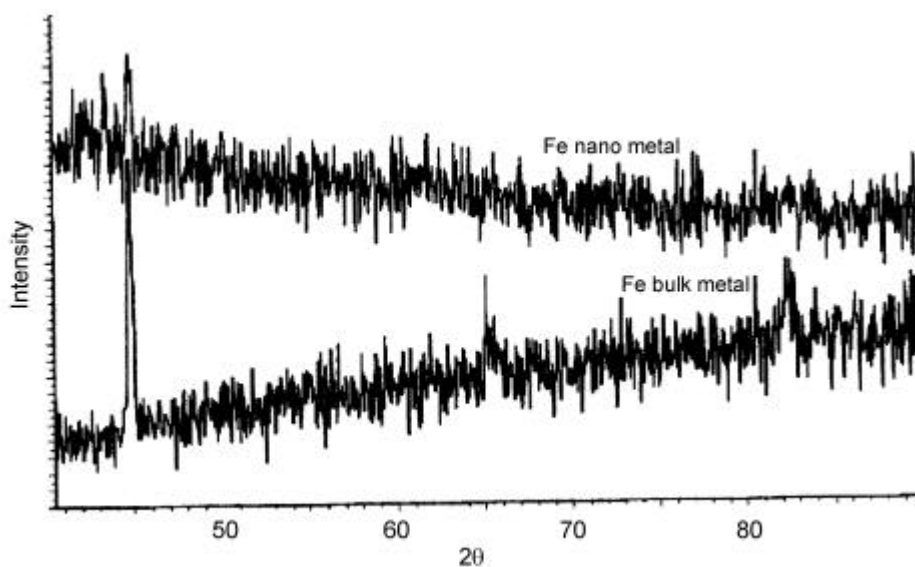


**Figure 6.** X-ray diffraction pattern of bulk iron metal is compared with iron nanoparticles obtained by the EEW technique.

3.3 *Iron*

Figure 5 shows the 3-dimensional projection of AFM data collected for nano-crystalline iron particles dispersed on Si (100).<sup>8</sup> The AFM picture shows distribution of uniform particles interspersed with some large clusters. A measurement of the diameters of several particles were carried out to infer particle sizes in the range 10–50 nm.

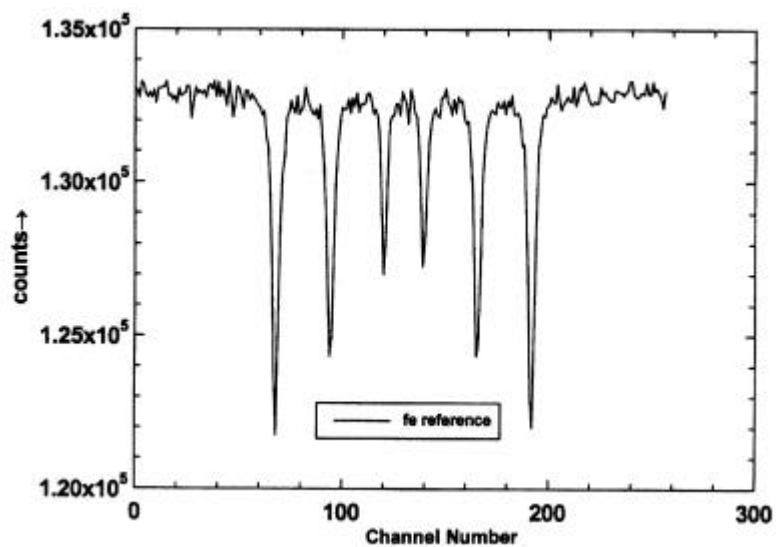


**Figure 7.** Mossbauer spectrum of bulk iron metal. The velocity = 0 position is at channel number 128.

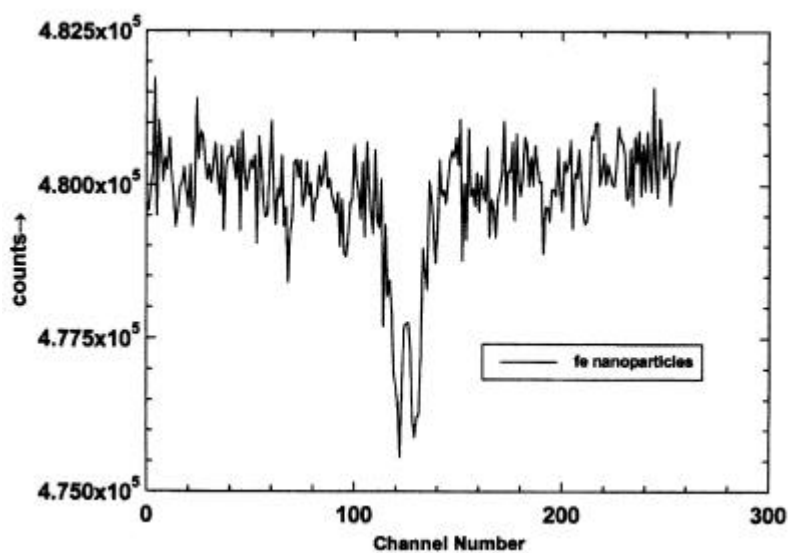
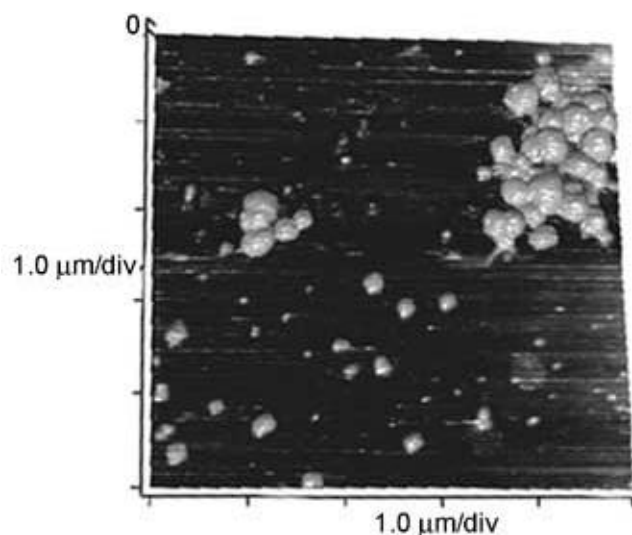


**Figure 8.** Mossbauer spectrum of nanoparticles of iron obtained by the EEW technique. The velocity = 0 position is at channel number 128.

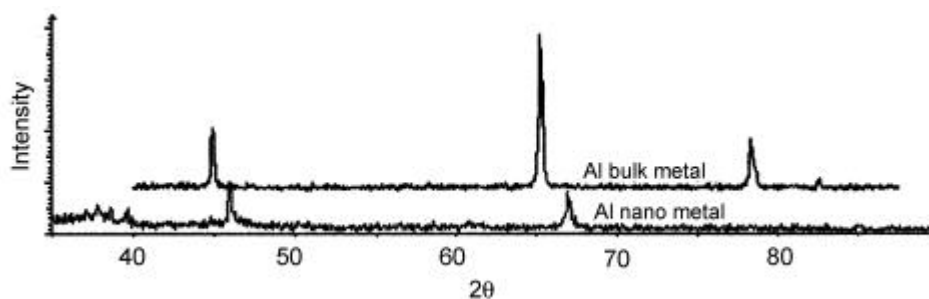


Figure 6 shows the XRD pattern recorded for bulk iron as a  $q$ - $2q$  plot scanning from  $44$ – $90^\circ$  generating the lines (110), (200), (211) at  $2q=44.8^\circ$ ,  $65.0^\circ$  and  $82.0^\circ$  respectively. For the nano-iron sample held onto the paper matrix as stated above, an XRD pattern was generated as a  $q$ - $2q$  plot scanning from  $44$ – $90^\circ$ . In this case only the most intense peak appears at  $44.8^\circ$  but the other two does not. The predominance of the (110) line in XRD indicates reorientation of the nanoparticle grains preferentially in one direction as against the random orientation of grains in the bulk material.

In figure 7 we present the Mossbauer spectrum of an iron foil showing the typical 6-line spectrum of a ferromagnetic material. However, the nanoparticles display a collapse in the ferromagnetic state yielding a Mossbauer doublet as shown in figure 8. The doublet is a result of the evolution of paramagnetism in the iron nanoparticles and can be compared to the particle size-dependant evolution of superparamagnetism in  $\alpha\text{-Fe}_2\text{O}_3$ , for particle sizes less than 15 nm, as reported by Greenwood and Gibbs.<sup>9</sup>



**Figure 9.** A contact mode AFM picture showing the aluminium nanoparticles as a 3-dimensional projection. The height axis ( $Z$  axis) is perpendicular to the plane of the paper.



**Figure 10.** X-ray diffraction pattern of bulk aluminium metal is compared with aluminium nanoparticles obtained by the EEW technique.

### 3.4 Aluminium

Figure 9 shows the 3-dimensional projection of AFM data collected for nano-crystalline aluminium particles dispersed on Si (100).<sup>8</sup> The AFM results show clusters of spherical particles together with well-defined singles. A typical particle is chosen for the size measurement by drawing a line across to measure the diameter. Several particles were investigated to infer particle sizes in the range 40–150 nm.

Figure 10 shows the XRD pattern recorded for bulk aluminium as a  $q$ - $2q$  plot scanning from 40–85° generating the lines (200), (220), (311), (222) at  $2q = 45.2^\circ$ ,  $65.4^\circ$ ,  $78.4^\circ$  and  $82.6^\circ$  respectively. For nano-aluminium the first peak was observed at  $2q = 46.1^\circ$  and the second peak was observed at  $2q = 66.8^\circ$ . No peaks were observed after that. These peaks were comparatively broadened with respect to those of bulk aluminium. The position of these lines for the nano-aluminium are distinct from those of the bulk material indicating a highly distorted aluminium lattice in the nanomaterial.

## 4. Conclusion

We have shown that nanoparticles can be made from conducting parent materials which can be shaped in the form of a wire/plate, employing the electro explosion of wire method. In this case both electrodes produce the particles. The dominant mechanism here is spark explosion, which is an adaptation of the electro-explosion of wires phenomena. The spark is achieved in a medium whose polarizability is of no consequence for the process and hence any dense medium can be employed.

## References

1. Azevedo R, Graneau P, Millet C and Graneau N 1986 *Phys. Lett.* **117** 101
2. Shelkovenko T A, Pikuz S A, Mingaleev, A R and Hammer D A 1999 *Rev. Sci. Instrum.* **70** 667
3. Vlastós A E 1973 *J. Appl. Phys.* **44** 106
4. Pikuz S A, Shelkovenko T A, Sinars D B, Greenly J B, Dimant Y S and Hammer D A 1999 *Phys. Rev. Lett.* **83** 4313
5. Graneau P 1983 *Phys. Lett.* **A97** 253
6. Aspden H 1987 *Phys. Lett.* **A120** 80
7. Ivezjæ T 1991 *Phys. Rev.* **A44** 2682
8. Sen P, Ghosh Joyee, Kumar Prashant, Abdullah Alqudami and Vandana 2003 (patent applied for)
9. Greenwood N N and Gibbs T C 1971 *Mossbauer spectroscopy* (London: Chapman & Hall) p. 246